Revista Brasileira de Geofísica
RBGf
Brazilian Journal of Geophysics

Revista Brasileira de Geofísica (2018) 36(4):559-567

ISSN 0102-261X
www.scielo.br/rbg

THE INFLUENCE OF MAGNITUDES TYPES IN THE NONEXTENSIVITY APPLIED AT THE CIRCUM-PACIFIC SUBDUCTION ZONES

Thaís Machado Scherrer[1,2], George Sand França[1], Raimundo Silva[3], Daniel Brito de Freitas[4] and Carlos da Silva Vilar[5]

ABSTRACT. Following our own previous work, we reanalyze the nonextensive behavior over the circum-Pacific subduction zones evaluating the impact of using different types of magnitudes in the results. We used the same data source and time interval of our previous work, the NEIC catalog in the years between 2001 and 2010. Even considering different data sets, the correlation between q and the subduction zone asperity is perceptible, but the values found for the nonextensive parameter in the considered data sets presents an expressive variation. The data set with surface magnitude exhibits the best adjustments.

Keywords: nonextensivity, seismicity, Solid Earth, earthquake.

RESUMO. No mesmo caminho do nosso trabalho anterior, reanalisamos o comportamento não extensivo sobre as zonas de subducção do círculo de fogo do Pacífico, avaliando o impacto do uso de diferentes tipos de magnitude nos resultados. Utilizamos o mesmo intervalo de dados e fonte de nosso trabalho anterior, do catálogo NEIC entre os anos 2001 e 2010. Mesmo considerando diferentes conjuntos de dados, a correlação entre q e a aspereza das zonas de subducção é perceptível, mas os valores encontrados para o parâmetro não extensivo nos conjuntos de dados considerados apresentam uma variação expressiva. O conjunto de dados com magnitude de superfície exibe os melhores ajustes.

Palavras-chave: não extensividade, sismicidade, Terra Sólida, terremoto.

[1]Universidade de Brasília, Observatório Sismológico, Campus Darcy Ribeiro, SG 13, Asa Norte, Brasília, DF, Brazil - E-mails: t_scherrer@yahoo.com.br, georgesand@unb.br
[2]Conselho Nacional de Desenvolvimento Científico e Tecnológico – CNPq, SHIS QI 01, Conj. B, Bl. A-D, Edifício Santos Dumont, Lago Sul, 71.605-001, Brasília, DF, Brazil
[3]Universidade Federal do Rio Grande do Norte, Departamento de Física, 59072-970 Natal, RN, Brazil – E-mail: raimundosilva@dfte.ufrn.br
[4]Universidade Federal do Ceará, Departamento de Física, Caixa Postal 6030, Campus do Pici, 60455-900 Fortaleza, CE, Brazil – E-mail: danielbrito@fisica.ufc.br
[5]Universidade Federal da Bahia, Instituto de Física, Campus Universitário de Ondina 40210-340 Salvador, BA, Brazil – E-mail: vilar@ufba.br

INTRODUCTION

In our previous work (Scherrer et al., 2015) we presented a brief review about the use of Tsallis Statistics in Seismology and used a model based on this approach, developed by Sotolongo-Costa & Posadas (2004) and revised by Silva et al. (2006), to relate the nonextensive parameter with the subduction zones along the Pacific Ring of Fire as described by Lay & Kanamori (1981). For that study, we used data of 142,280 events in magnitude interval $1 \leq M \leq 9$, taken from the National Earthquakes Information Center Catalog (NEIC-USGS) during the 2001 and 2010 periodo. We followed the NEIC automatic ranking, independent of the magnitude type (M_W, m_b, M_S, M_L, among others) used to measure each event. We consider at that time that this would makes no significant impact on the final result because, in general, the differences between different magnitudes types are small. In this paper we considered four different types of magnitude (M_W, m_b, M_S, M_L) independently and made the nonextensive model fitting on each individual data set verifying a significant variation from what was found in Scherrer et al. (2015).

NONEXTENSIVE FORMALISM

Starting from Boltzmann-Gibbs entropy, (Tsallis, 1988, 1995a,b, 2009) developed a different model that can be applied to systems in non-equilibrium state, complex behavior and fractal pattern – characteristics present in earthquakes and geological faults. The entropy in this model is calculated as

$$S_q = -k_B \sum_{i=1}^{W} p_i^q \, ln_q \, p_i, \tag{1}$$

where k_B is Boltzman's constant, p_i is a set of probabilities and W is the total number of microscopic configurations. q is the nonextensive parameter, and q-logarithmic function above is defined by

$$ln_q = (1-q)^{-1}(p^{1-q} - 1) \quad p > 0. \tag{2}$$

It's easily verified that this is a generalization of Boltzmann-Gibbs entropy, as in the limit $q = 1$ for eq. 1, we recover the classical model,

$$S_q = -k_B \frac{1 - \sum_{i=1}^{W} p_i^q}{q-1}. \tag{3}$$

In order to investigate the impact of using different types of magnitudes, we used the same model revised by Silva et al. (2006) for earthquakes, in which the q-entropy is denoted by

$$S_q = -k_B \int p^q(\sigma) \, ln_q \, p(\sigma) d\sigma, \tag{4}$$

where k_B is the Boltzmann constant and; $p(\sigma)$ is the probability of finding a fragment of surface σ. In the same way, when $q = 1$, the equation becomes the entropy definition by Boltzmann-Gibbs. The relation of q-entropy with the number of earthquakes is also demonstrated by Silva et al. (2006). When considered that energy scale $\varepsilon \sim r^3$, i.e. the energy distribution from earthquakes reflects the volumetric distribution of the fragments between plates, the model is given by:

$$log(N_m) = logN + \left(\frac{2-q}{1-q}\right) log\left[1 - \left(\frac{1-q}{2-q}\right)\left(\frac{10^{2m}}{a^{2/3}}\right)\right], \tag{5}$$

where $N > m$ is the number of earthquakes with magnitude larger than m, N is the total number of earthquakes and a is the proportionality constant between the fragments volume and released energy.

THE ASPERITY MODEL AND THE CIRCUM-PACIFIC SUBDUCTION ZONES

A more complete description of the zones can be found in Lay & Kanamori (1981), Kanamori, 1986, Müller & Landgrebe (2012), Uyeda (2013) and Scherrer et al. (2015). Here we will just present the basic information to identify the areas analyzed and allow a clearly understanding of the section V. At the Table 1, we present the limits considered for each area shown in Figure 1.

A briefly description of each zone is shown in Table 2 and featured in Figure 2. As described in Lay & Kanamori (1981) and Kanamori (1986):

- In the Chile-type behavior (zone 1), the lithospheric plates are strongly coupled, and the asperity distribution is basically uniform over the contact area, because of that, rupture occurs in great events. Sediments are scraped off on subduction and form an accretionary prism, what causes excess trend sediments. The trench and the dip angle of Wadati-Benioff are usually shallow.

- For Aleutians-type (zone 2- considering the Western part), the asperities are comparatively large, but they are surrounded by weak zones. The relatively homogeneity causes some large ruptures but smaller ruptures also occur, possibly as doublets.

- Because of the relatively small size of asperities and heterogeneities in Kuriles-type zones (zone 3), there is an inhibition of large rupture development generating complicated ruptures and foreshock-aftershock activity.

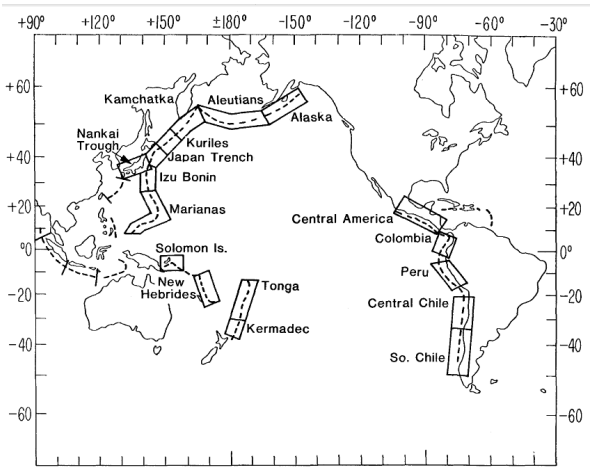

Figure 1 – Circum-Pacific Subduction Zones, indicating areas considered in Lay & Kanamori (1981), and Figure 5.1.

Table 1 – Areas considered in this study, from Scherrer et al. (2015).

Area	Latitude		Longitude	
	North	South	East	West
Tonga	-12	-30	-168	177
Kermadec	-30	-42	-174	172
New Hebrides	-9	-24	175	163
Solomon Islands	-2	-20	160	145
Marianas	28	8	150	135
Kuriles	48	44	158	145
Kamchatka	58	48	166	155
Aleutians	54	48	-165	-166
Central America	21	7	-74	-108
Colombia	7	-5	-74	-82
Peru	-5	-17	-68	-85
Central Chile	-17	-35	-65	-78
South Chile	-35	-49	-68	-78

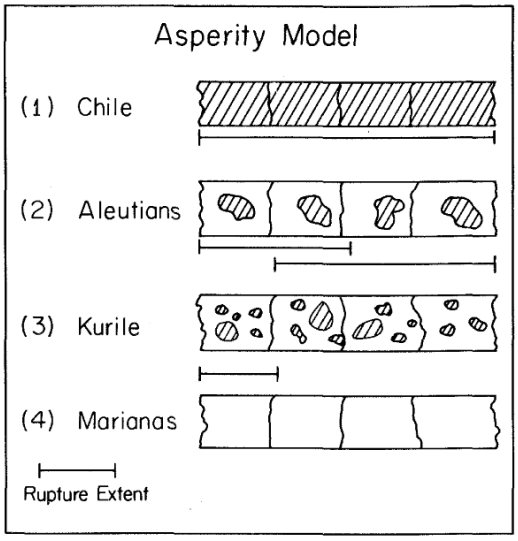

Figure 2 – An asperity model indicating the different nature of stress distribution in each subduction zone category. The hatched areas indicate the zones of strong coupling. From Lay & Kanamori (1981), and Figure 5.4.

Table 2 – Subduction zones characteristics, from Lay & Kanamori (1981), and Figure 5.2, with few alterations. In this study the Aleutians were considered as one area, including western and central regions.

Categories	Areas	Characteristics
1	Southern Chile, Southern Kamchatka, Alaska, Central Aleutians	Regular occurrence of great ruptures (500 km long). Large amount of seismic slip.
2	Western Aleutians (Rat Islands), Colombia, Nankai Trough, Solomon Islands	Variations in rupture extent, with occasional rupture 500 km long. Close clustering of large events and doublets.
2-3	New Hebrides, Central America	Intermediate size and small events with no great earthquakes, but clustering of activity.
3	Kuriles Islands, Northeast Japan Trench, Peru, Central Chile	Repeated ruptures over limited zones. No great events. Large component of aseismic slip, or subducting ridges.
4	Marianas, Izu-Bonin, Southeast Japan Trench, Tonga, Kermadec	Large earthquakes are infrequent or absent. Back-arc spreading and large amounts of aseismic slip are inferred.

- The last category (Marianas-type-zone 4) is characterized by no large asperities, so weak coupling and no large earthquakes. There is a heterogeneous contact plane that decreases the strength of mechanical coupling; it is called "host-and-graben structures". The trench and the dip angle of Wadati-Benioff are usually steeper. The back-arc basin is commonly found for this type of subduction zones.

MAGNITUDE TYPES

A wider description of the types of magnitude can be found in Kanamori (1983) and Båth (1981), including the mathematical relations between them. We present just the basic characteristics and limitations of the most commonly used and also considered in this work.

The first magnitude scale in Seismology was developed by Richter (1935) and called the local magnitude (M_L) or Richter magnitude. It's measured by records of the standard Wood-Anderson torsion seismograph and it's influenced by each region attenuation characteristics. It's applicable just until 600 km of distance. In 1945, Gutenberg (1945b,a) introduced more two scales:

- Surface-wave magnitude (M_S), considering shallow earthquakes, defined by:

$$M_s = logA_S + 1.656\, log\Delta^\circ + 1.818, \qquad (6)$$

  where A_S is the surface wave amplitude and Δ° is the distance from the shallow epicenter in degrees.

- And the body-wave magnitude, m_b, that considered a wave group with different seismic phases and could be used to measure shallow and deep events, calculated by:

$$m_b = log\frac{A_b}{T} + Q + C, \qquad (7)$$

  where A_b is the wave maximum amplitude, T is the wave period, Q is an attenuation factor and C is the station correction. But, this estimation can produce anomaly high values for distances under 2000 km in continental regions of lower seismicity (Berrocal et al., 1984).

Both scales have limited range and applicability and are saturated when the magnitude is higher than 8.

The moment magnitude (M_W) scale, based on the concept of earthquake seismic moment, which is equal to the rigidity of the Earth multiplied by the average amount of slip on the fault and the size of the area that slipped, can be useful to measure all sizes of earthquakes but is more difficult to compute than the other types.

$$M_W = \frac{2}{3}\, log_{10}(M_0) - 6.0, \qquad (8)$$

where M_0 is the seismic moment in *Nm*. The constant values in the equation are chosen to achieve consistency with the magnitude values produced by M_L and M_S.

These scales were conceived as intercalibrated and should yield approximately the same value for any given earthquake, however, Kanamori (1983) points out that, "because of the difference in the type of seismic waves and wave period, complete calibration cannot be made. That's not necessarily a problem, since different scales may represent fundamentally different properties of the source".

RESULTS AND DISCUSSION

As shown in Scherrer et al. (2015), we found good adjustments for the catalog data set (indicated here by the subscription cat), but now the original data for each area was adjusted, considering also new sets as described: all events considering the following priority of magnitude types – M_W, m_b, M_S, M_L, M_D, M_G (subscripted as *pr*), and events measured by magnitudes M_W, M_S, m_b and M_L separately. Considering the similarity between this model and the modified Gutenberg-Richter law, we also calculated the parameter b, as was described for Sarlis et al. (2010):

$$b = 2(2-q)/(q-1). \qquad (9)$$

Results are shown in Tables 3 to 5 and Figures 3-6. The q-values found presented a wider range (specially for the fitting with M_L), from 1.18 to 1.69. In all the adjustments, zone 1 has q-values typically higher. For the data sets cat, pr, M_S and m_b, the areas from zone 4 has typically lower values. However, it's necessary to stand out that the range between the higher and lower q-value is smaller in catalog and mb data sets. But again, it was hard to categorize the intermediate zones. Also, the q-value for Kamchatka region for all data sets doesn't follow the values for the other areas in subduction zone 1.

As can be seen in Tables 3-5, in each set and for each area even in just a 10 years period a significant number of events was considered in the analysis, the only exception was M_W.

Unfortunately even so, we considered it's not possible to reach a plausible conclusion with this data set. Each data set presents very different inclination of the curves, but inside the same data set these inclinations are similar. In general, the M_S data set presented the best adjustments.

Table 3 – Values to q and b, calculated with magnitude as the catalog presents, considering magnitudes in priority: M_W, m_b , M_S, M_L, M_D, M_G. sd is standard deviation.

Subduction Zone Category	Area	q_{cat}	sd	b_{cat}	number of events	q_{pr}	sd	b_{pr}	number of events
1	South Chile	1.6978	0.0091	0.8661	4038	1.509	0.0100	1.9331	3832
1	Alaska	1.6656	0.0055	1.0050	5671	1.448	0.0085	2.4679	4763
1	Kamchatka	1.6448	0.0041	1.1019	5648	1.419	0.0068	2.7730	5648
1-2	Aleutians	1.6746	0.0035	0.9646	10810	1.444	0.0082	2.5015	10288
2	Colombia	1.6548	0.0088	1.0543	2309	1.435	0.0075	2.5968	2304
2	Solomon Islands	1.6507	0.0013	1.0737	13125	1.426	0.0026	2.6913	13125
2-3	New Hebrides	1.6645	0.0023	1.0097	9818	1.455	0.0035	2.3952	9768
2-3	Central America	1.6341	0.0038	1.1539	19488	1.441	0.0051	2.5301	9043
3	Kuriles	1.6557	0.0025	1.0503	7428	1.434	0.0040	2.6088	5306
3	Central Chile	1.6549	0.0026	1.0540	27106	1.428	0.0052	2.6743	24642
3	Peru	1.6560	0.0048	1.0489	2331	1.435	0.0050	2.5932	2311
4	Kermadec	1.6128	0.0040	1.2638	21655	1.388	0.0038	3.1612	21302
4	Marianas	1.6350	0.0028	1.1499	8560	1.427	0.0031	2.6883	8486
4	Tonga	1.6340	0.0037	1.1546	23462	1.433	0.0039	2.6154	23462

Table 4 – Values to q and b, calculated only with M_S and only with M_W. The subduction zones for each area are indicated and sd is standard deviation.

Subduction Zone Category	Area	q_S	sd	b_S	number of events	q_W	sd	b_W	number of events
1	South Chile	1.610	0.0082	1.2804	209	1.593	0.0210	1.3706	89
1	Alaska	1.547	0.0034	1.6577	335	1.329	0.0140	4.0755	28
1	Kamchatka	1.521	0.0038	1.8394	599	1.481	0.0280	2.1557	21
1-2	Aleutians	1.537	0.0058	1.7265	1200	1.437	0.0230	2.5788	67
2	Colombia	1.502	0.0100	1.9827	753	1.657	0.0590	1.0437	12
2	Solomon Islands	1.540	0.0059	1.7059	2809	1.487	0.0082	2.1107	159
2-3	New Hebrides	1.541	0.0045	1.6945	2601	1.536	0.0094	1.7287	203
2-3	Central America	1.521	0.0020	1.8379	1765	1.483	0.0100	2.1410	444
3	Kuriles	1.554	0.0042	1.6071	1309	1.524	0.0110	1.8195	48
3	Central Chile	1.537	0.0051	1.7227	944	1.483	0.0087	2.1410	444
3	Peru	1.578	0.0071	1.4591	652	1.365	0.0150	3.4747	36
4	Kermadec	1.506	0.0038	1.9505	1162	1.400	0.0290	2.9946	52
4	Marianas	1.526	0.0018	1.8014	1558	1.534	0.0065	1.7476	99
4	Tonga	1.508	0.0045	1.9374	3091	1.500	0.0120	1.9990	297

Table 5 – Values to q and b, calculated only with m_b and only with M_L. The subduction zones for each area are indicated and sd is standard deviation.

Subduction Zone Category	Area	q_B	sd	b_B	number of events	q_L	sd	b_L	number of events
1	South Chile	1.421	0.0088	2.7509	1517	1.502	0.01062	1.9878	2482
1	Alaska	1.399	0.0064	3.0152	1427	1.615	0.00455	1.2515	3476
1	Kamchatka	1.434	0.0043	2.6069	2351	1.183	0.00744	8.9487	3311
1-2	Aleutians	1.404	0.0100	2.9559	4233	1.427	0.00482	2.6802	6673
2	Colombia	1.415	0.0059	2.8216	2298	1.516	0.02232	1.8782	64
2	Solomon Islands	1.384	0.0090	3.2119	13119	1.348	0.00729	3.7409	1255
2-3	New Hebrides	1.386	0.0039	3.1865	9102	1.420	0.00893	2.7658	948
2-3	Central America	1.447	0.0073	2.4696	6557	1.312	0.00811	4.4133	2430
3	Kuriles	1.419	0.0027	2.7759	5291	1.209	0.00495	7.5662	259
3	Central Chile	1.407	0.0035	2.9128	7579	1.406	0.00414	2.9307	17548
3	Peru	1.426	0.0041	2.6968	2301	1.410	0.00914	2.8746	195
4	Kermadec	1.372	0.0029	3.3785	6645	1.320	0.00472	4.2584	15257
4	Marianas	1.411	0.0022	2.8671	8479	1.357	0.00742	3.5968	225
4	Tonga	1.401	0.0030	2.9814	23448	1.435	0.02110	2.5996	504

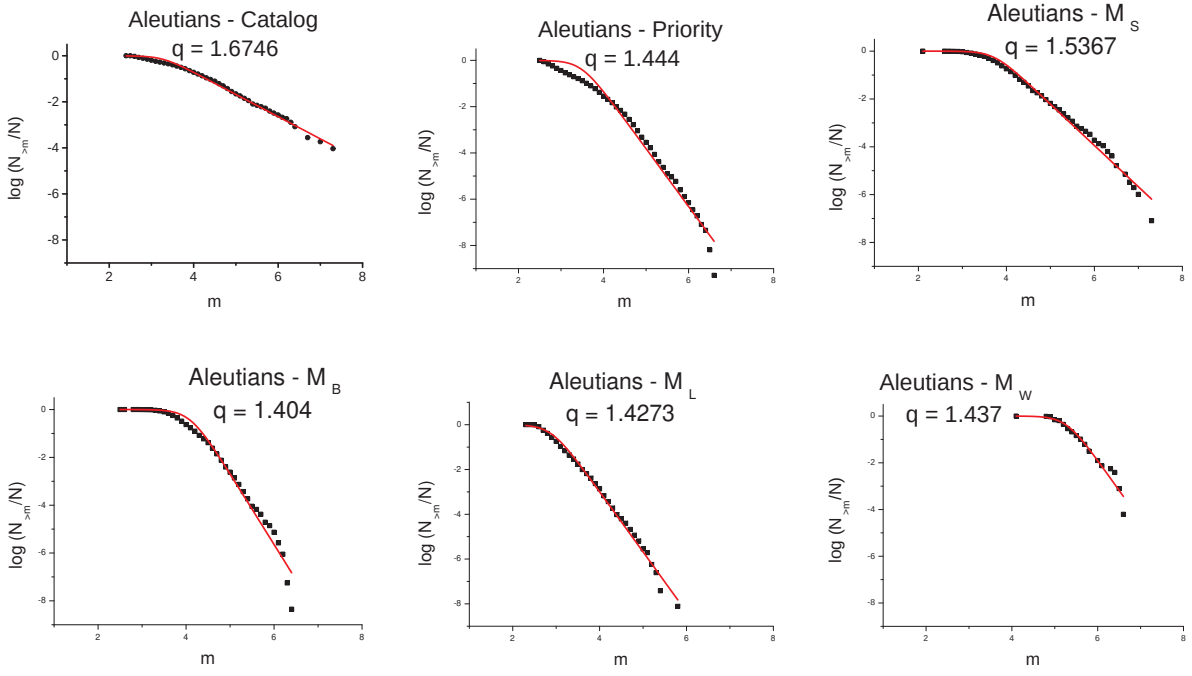

Figure 3 – The relative cumulative number of earthquakes as a function of the magnitude m for Aleutians, representing zone 1. We show the graphics for using catalog magnitudes, priority magnitudes, M_S, m_b (M_B), M_L, M_W, respectively.

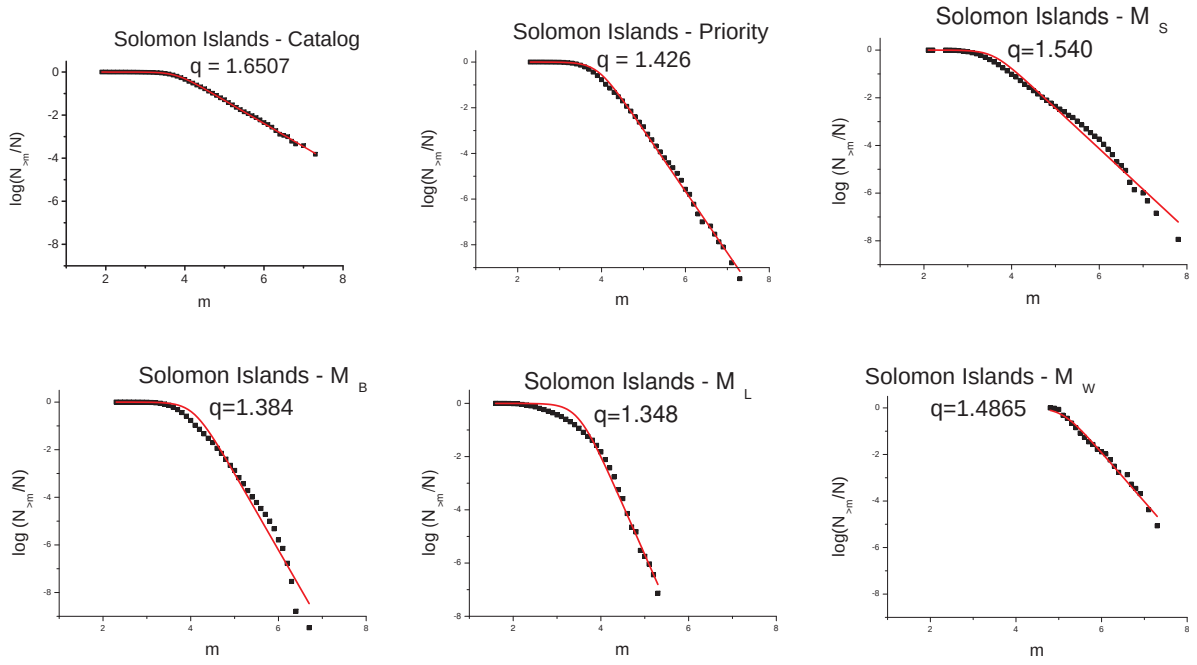

Figure 4 – The relative cumulative number of earthquakes as a function of the magnitude m for Solomon Islands, representing zone 2. We show the graphics for using catalog magnitudes, priority magnitudes, M_S, m_b (M_B), M_L, M_W, respectively.

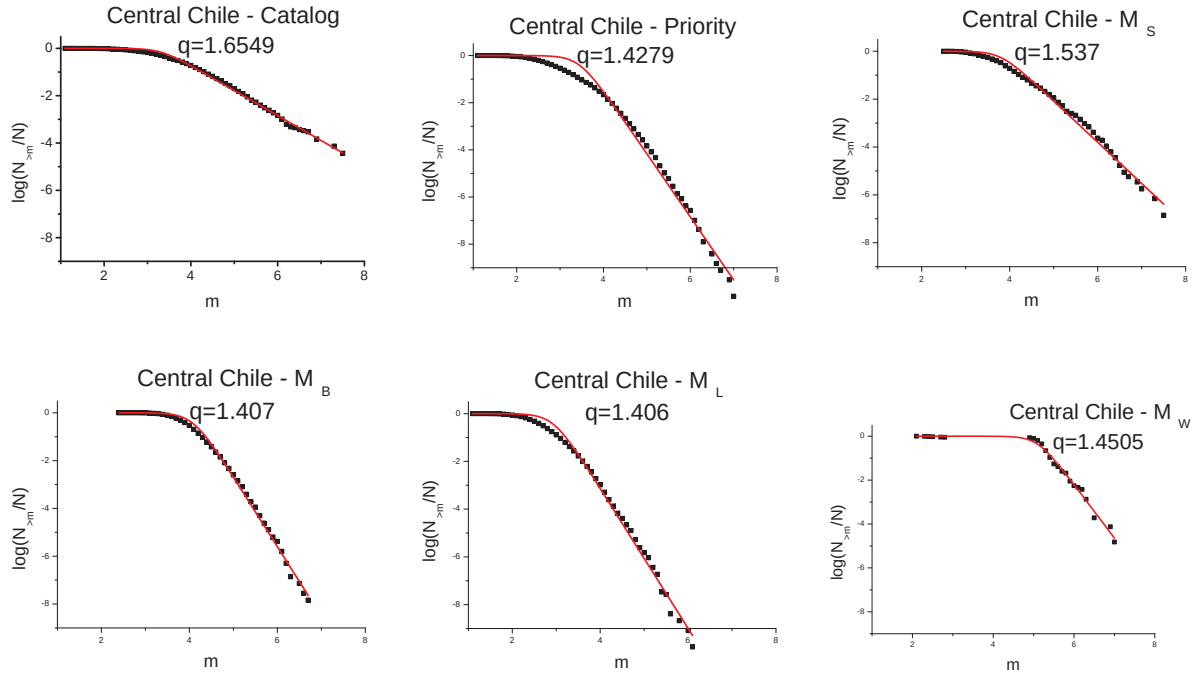

Figure 5 – The relative cumulative number of earthquakes as a function of the magnitude m for Central Chile, representing zone 3. We show the graphics for using catalog magnitudes, priority magnitudes, M_S, m_b (M_B), M_L, M_W, respectively.

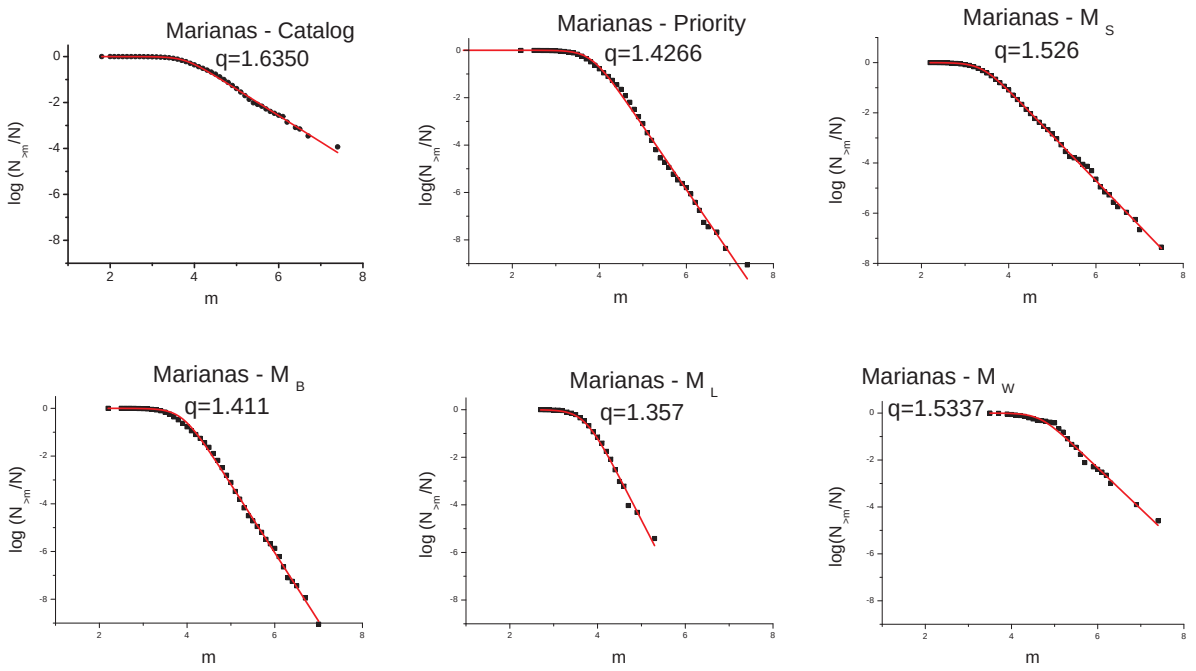

Figure 6 – The relative cumulative number of earthquakes as a function of the magnitude m for Marianas, representing zone 4. We show the graphics for using catalog magnitudes, priority magnitudes, M_S, m_b (M_B), M_L, M_W, respectively.

The b values are inconsistent with those estimated by the Gutenberg-Ritchter law, exactly using the prior procedures and the isolated magnitudes. Of course, the decrease in the number of events impacts both q and b estimates. Those b values obtained from q analysis are influenced by the saturation effect. In the example of M_L, we can see that q_L shows very low values, and so b estimates are influenced. Another important point is the data completeness, which affects the Gutenberg-Ritchter law and for the nonextensive it is not an important factor. Therefore, the values of q for different magnitudes, better represents regional trends behavior but do not represent the correlation with the value of b by Sarlis et al. (2010).

CONCLUSIONS

Other than expected, we observed a great variation of the q-value calculated considering different magnitudes types while the cumulative distribution of the data presented very distinct inclinations for each case. In general, q_{cat} and q_S are those that better correlate with the subduction zones, zone 1 presents higher values and zone 4 lower values. But for the intermediate areas it's still not possible to separate the categories considering these parameters. The influence of coupling for the nonextensive parameter is reaffirmed. The good adjustment with q_S may be due to the relevance of the fragmentation process in nonextensive behavior. The calculation with mb also presents a good correlation with the subduction zones.

ACKNOWLEDGMENTS

The authors thank anonymous referees for careful revision and positive criticism, which greatly improved our work. GSF and RS thank CNPq for their PQ grands (307251/2016-0 and 303613/2015-7, respectively).

REFERENCES

BÅTH M. 1981. Earthquake Magnitude – Recent Research and Current Trends. Earth-Science Reviews, 17: 315–398.

BERROCAL J, ASSUMPÇÃO M, ANTEZANA R, ORTEGA R, FRANÇA H, DIAS NETO CM & VELOSO JAV. 1984. Sismicidade do Brasil. Instituto Astronômico e Geofísico (Universidade de São Paulo) and Comissão Nacional de Energia Nuclear. São Paulo, Brazil. 320 pp.

GUTENBERG B. 1945a. Amplitudes of P, PP, and S and magnitude of shallow earthquakes. Bull. Seismol. Soc. Am., 35: 57–69.

GUTENBERG B. 1945b. Amplitudes of surface waves and magnitudes of shallow earthquakes. Bull. Seismol. Soc. Am., 35: 3–12.

KANAMORI H. 1983. Magnitude Scale an Quantification of Earthquakes. Tectonophysics, 93: 185–199.

KANAMORI H. 1986. Rupture Process of Suduction-Zone Earthquakes. Annu. Rev. Earth Planet. Sci., 14: 293–322.

LAY T & KANAMORI H. 1981. An asperity model of large earthquake sequences. Earthquake Prediction. Maurice Ewing Series, 4: 579–592.

MÜLLER RD & LANDGREBE TCW. 2012. The link between great earthquakes and the subduction of oceanic fracture zones. Solid Earth, 3: 447–465.

RICHTER C. 1935. An instrumental earthquake magnitude scale. Bull. Seismol. Soc. Am., 25: 1-32.

SARLIS NV, SKORDAS ES & VAROTSOS PA. 2010. Nonextensivity and natural time: The case of seismicity. Phys. Rev. E, 82: 021110. doi: 10.1103/PhysRevE.82.021110.

SCHERRER TM, FRANÇA GS, SILVA R, DE FREITAS DB & VILAR CS. 2015. Nonextensivity at the Circum-Pacific Subduction Zones – Preliminary Studies. Physica A, 246: 63–71. doi: 10.1016/j.physa.2014.12.038.

SILVA R, VILAR FG, CS & JS A. 2006. Nonextensive models for earthquakes. Phys. Rev. E, 73. 5 pp.

SOTOLONGO-COSTA O & POSADAS A. 2004. Fragment-Asperity Interaction Model for Earthquakes. Phys. Rev. Lett., 92: 048501–048504.

TSALLIS C. 1988. Possible generalization of Boltzmann-Gibbs statistics. J. Stat. Phys., 52: 479–487.

TSALLIS C. 1995a. Nonextensive thermostatistics: brief review and comments. Physica A, 221: 277–290.

TSALLIS C. 1995b. Some comments on Boltzmann-Gibbs statistical mechanics. Chaos, Solitons and Fractals, 6: 539–559.

TSALLIS C. 2009. Introduction to Nonextensive Statistical Mechanics – Aproaching a Complex World. Springer, New York. 382 pp.

UYEDA S. 2013. On Earthquake Prediction in Japan. Proc. Jpn. Acad. Ser. B. Phys. Biol. Sci., 89(9): 391–400.

Recebido em 29 setembro, 2018 / Aceito em 10 dezembro, 2018

Received on September 29, 2018 / Accepted on December 10, 2018